Eur. Phys. J. B **7**, 339–345 (1999)

THE EUROPEAN PHYSICAL JOURNAL B

EDP Sciences

X-ray scattering by nano-particles within granular thin films, investigation by grazing angle X-ray reflectometry

M. Mâaza[1,2], A. Gibaud[1,a], C. Sella[3], B. Pardo[2], F. Dunsteter[5], J. Corno[2], F. Bridou[2], G. Vignaud[1], A. Désert[1], and A. Menelle[4]

[1] Laboratoire de Physique de l'État Condensé[b], Université du Maine, Faculté des Sciences, 72085 Le Mans Cedex 09, France
[2] Institut d'Optique Théorique & Appliquée, Bâtiment 503, Université Paris-Sud, 91403 Orsay Cedex, France
[3] Laboratoire d'Optique des Solides, Université Paris VI, Paris, France
[4] Laboratoire Léon Brillouin[c], CEA Saclay, 91191 Gif-sur-Yvette Cedex, France
[5] Laboratoire des Solides Irradiés, École Polytechnique, Palaiseau, France

Received: 19 February 1998 / Accepted: 25 August 1998

Abstract. It is shown here that the observation of the phenomenon of like small angle scattering of X-rays in very thin heterogeneous films, can be made comparatively easily by using grazing angle reflectometry of X-rays. The feasibility was achieved with co-sputtered thin films of approximately 600 Å thickness, made up by crystalline platinum clusters embedded in an amorphous alumina matrix. The experimental reflectivity profiles are simulated by the intensity superposition of two components: (i) the specular part caused by the usual interference phenomenon between the partial waves reflected from the air-film and film-substrate interfaces, and (ii) the like-small angle scattering part due to diffraction by platinum clusters. It is found that the shape of such clusters is spherical characterized by mean values of diameter $\langle \phi_c \rangle$ and inter-cluster distance $\langle S_c \rangle$ of the order 29 Å and 45 Å respectively with standard deviations σ_ϕ and σ_S of the order of 3 Å. Such an observation of both the interference and diffraction phenomena indicates that the thin granular film exhibits both its continuous and heterogeneous aspects together.

PACS. 61.10.Kw X-ray reflectometry (surfaces, interfaces, films) – 61.46.+w Clusters, nanoparticles, and nanocrystalline materials – 68.55.-a Thin film structure and morphology

1 Introduction

Small angle scattering of X-rays (SAXS) or neutrons (SANS) is a useful method for investigating finely divided materials in nanometric scale within condensed matter. From such studies, where generally two phases coexist, much information can be obtained regarding the shape, size, distance between the sub microscopic particles and nuclear or magnetic correlation if any. According to their efficiency, SAXS and SANS are now, one of the most important methods because of their application to many scientific fields, such as solid-state physics, chemistry, materials science, polymers and biology [1]. This blooming follows a period of many years, starting soon after Guinier's effective inception of the field in 1939 [2], during which only a handful of dedicated scientists around the world kept work going in the theory and practice of SAXS [3,4]. Recently, the high resolution experiments due to the ultra-narrow reflections of perfect silicon crystals extended more the possibilities of both SAXS and SANS methods [5,6]. All of the previous SAXS and SANS experiments were performed in transmission geometry. Unfortunately, this configuration limits, the possibilities of these powerful methods in which the main constraints are: (i) the measurements are disturbed by the direct transmitted beam which is a background source, (ii) thick samples are required ($\geq$ 1 mm thickness), so 2D phenomena in very thin films could not be studied, and finally, (iii) this method is not really suitable to give information on the interfacial aspects, because the interfacial region is usually small compared to the bulk phases and thus gives only a small contribution to the volume scattering effect. To overcome such difficulties, surface scattering methods are developed and used to probe numerous surface phenomena [7–9].

The present contribution deals with the possibility of overcoming the former quoted limits of small angle scattering techniques, in the case of granular films of cermet type, by using grazing angle reflectometry of X-rays (GAXR) or neutrons (GANR). Indeed, due to their high sensitivity to surface and interface phenomena, points (ii) and (iii) could be licked by GAXR and GANR. It should be emphasized that the discussion within this paper is restricted to studying very thin granular films dealing essentially with heavy metallic heterogeneity embedded in a light matrix.

[a] e-mail: gibaud@aviion.univ-lemans.fr
[b] CNRS – UPRESA 6087
[c] CNRS – CEA

Before presenting our results, one can quote the two exceptional works concerning small angle scattering induced by surface scattering: Levine *et al.* [10] have shown that it is possible to use grazing angle X-ray scattering in non specular configuration to study the growth of thin discontinuous films. Likewise, out of specular configuration, the second paper by Naudon *et al.* exhibits the possibility of detecting Guinier-Preston zones induced at the surface of aged Ag-Al bulk samples [11]. The leading difference between these two former accomplishments (using GISAX) and the current one is that in our case, the experiments were performed on heterogeneous thin films; both thin film interference and heterogeneity' diffraction phenomena coexist together. A recent deep theoretical study on this kind of thin films performed by Rauscher *et al.* [12] using the distorted-wave Born approximation showed the possibility to observe SAXS within thin films presenting some particular density fluctuations. More accurately, they treated different real cases; among them one can quote the columnar structures and the isotropic density fluctuations with which we deal in the actual experiment results. In this sense, as it will be shown, our present experimental results can be considered as a confirmation of the validity of the theoretical work of Rauscher and co-workers.

To ascertain the possibility of observing this small angle X-ray (neutron) scattering in grazing angle reflection geometry with very thin inhomogeneous films as predicted by Rauscher *et al.*, three conditions are mainly required: (i) high contrast in the electron density between the clusters and the matrix, (ii) a low reflecting substrate and (iii) small interfacial roughness (air-thin film and thin film-substrate interfaces). In the present experimental contribution, ≈ 600 Å Pt-Al_2O_3 granular films are investigated. More precisely, these thin films consist of Pt clusters buried in an amorphous Al_2O_3 matrix. To obtain the characteristics of the Pt clusters *i.e.* average diameter $\langle \phi_c \rangle$, average separation distance $\langle S_c \rangle$ and their distributions (standard deviations σ_ϕ, σ_S), a representative model is proposed. The model is described in Section 2 whereas experimental results are discussed in Sections 3 and 4.

2 Theory and modelization

From a theoretical point of view, calculations of the scattering of X-ray (neutron) incident beam by a finely divide matter is simplest in two extreme cases, that where diffraction only is important as described by the theories of Rayleigh and Gans and, secondly, the case where refraction only is important, as covered by the theory of Von Nardorff. It was shown recently by Davis [13] using the Rytov approximation that these were indeed two limiting cases of a full treatment of the problem and were applicable according as the differential phase change DF between particle and matrix is much less or much greater than unity. As it will be shown, the two phenomena could coexist simultaneously in the case of granular thin films if investigated by grazing angle X-ray (cold neutron) reflectometry.

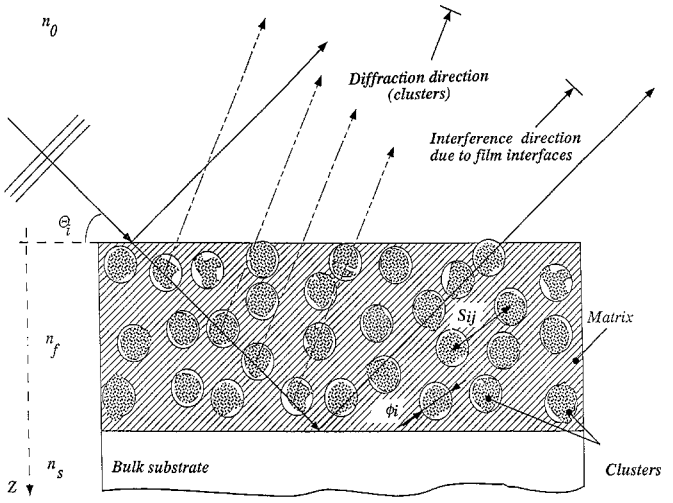

Fig. 1. Schematic cross-sectional view of a granular film of thickness D and an average refractive index n_f (n_s for substrate, n_0 for air). The heterogeneous film is considered as a set of quasi-spherical clusters embedded in a matrix.

Let us consider Figure 1; it represents a granular film of thickness D, made up by heavy quasi-spherical clusters characterized by a refractive index n_c, a scattering density δ_c, a mean diameter $\langle \phi_c \rangle$ and a mean inter-cluster distance $\langle S_c \rangle$ embedded in a light matrix characterized by a refractive index n_m and a scattering density d_m. From an optical point of view, the interaction of X-ray or neutron waves in such a medium with both clusters and matrix is described by a refractive index n_i expressed as

$$n_i = 1 - \frac{\lambda^2}{2\pi}\delta_i + i\beta_i \tag{1}$$

λ is the wavelength, $\delta_x = r_e \rho_{el}$ (for X-rays) and $\delta n = Nb$ (for cold neutrons), r_e the classical electron radius, ρ_{el} the electron density of each medium, b the mean scattering length for neutrons of each material and N the number density of nuclei, β is the absorption part. Just for the sake of simplification, we consider, herein after, the X-ray's notation. In the kinematical approximation, the amplitude of the scattered wave from the previous granular film, is the Fourier transform of the electron density in the film [3]:

$$A(\mathbf{Q}) = \int \rho\,(r)\, e^{-i\mathbf{Q}\cdot\mathbf{r}} dV. \tag{2}$$

In the following, $Q = \sqrt{(Q_x^2 + Q_y^2 + Q_z^2)}$ will be the modulus of the scattering vector $\mathbf{Q}$ and Q_x, Q_y, Q_z its components as shown in Figure 2a. The profile of the electron density in the granular thin films can be expressed as:

$$\rho(\mathbf{r}) = \{\rho_m(\mathbf{r}) + [\rho_c - \rho_m](\mathbf{r}) * \sum_k \delta(\mathbf{r} - \mathbf{r}_k)\} S(\mathbf{r}) \tag{3}$$

where the function $S(r)$ characterizes the limited dimensions of the thin film. This function is the product of three

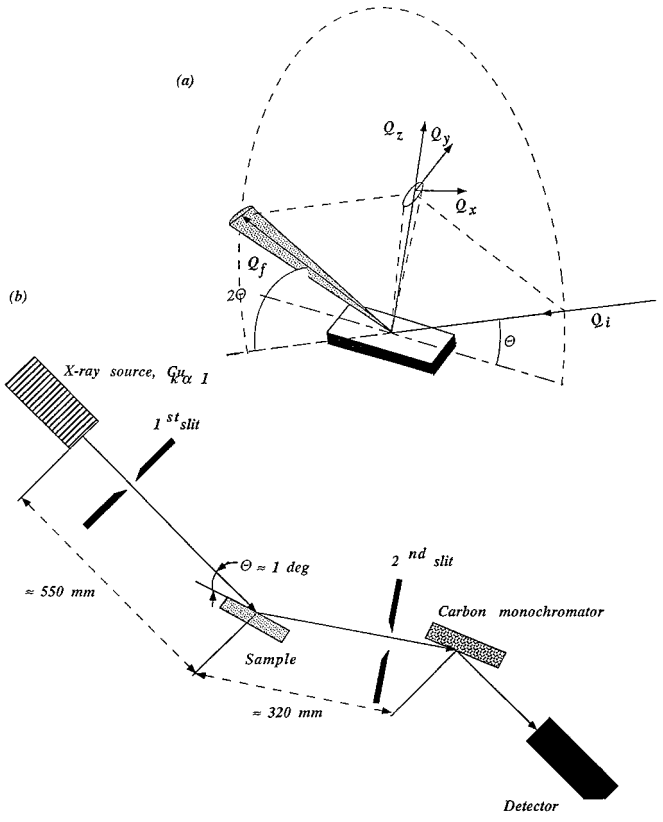

Fig. 2. (a) Grazing angle reflection geometry ($\theta \approx 1°$) and scattering vector components; (b) Layout of the used θ-2θ X-rays reflectometer: length source-sample = 550 mm, length sample-monochromator = 320 mm, width of the slits 40 to 200 μm, horizontal incident divergence = 0.32 mrad, max vertical incident divergence = 0.16 rad, horizontal reflected divergence = 0.16 mrad and vertical reflected divergence: according to sample size.

independent functions $S(\mathbf{r}) = h(x)k(y)l(z)$ in which z is limited by the extension of the film (z varying from 0 to D). Its Fourier transform is then:

$$TF[S(\mathbf{r})] = D\delta(Q_x)\delta(Q_y)\exp(iQzD/2)\sin c(Q_zD/2) = Z(\mathbf{Q}). \quad (4)$$

As the clusters are assumed to have a spherical shape, the Fourier transform of $[\rho_c - \rho_m](\mathbf{r})$ (Eqs. (2,3)), is related to the single-particle scattering function given by [3]:

$$TF[[\rho_c - \rho_m](\mathbf{r})] = 4\pi[\rho_c - \rho_m] \times R^3 3(\sin QR - QR\cos QR)/(QR)^3 = A_s(Q,R) \quad (5)$$

with $R = \langle\phi_c\rangle/2$ is the particle radius. As $TF[\sum\delta(\mathbf{r} - \mathbf{r}_k)] = \sum\exp[-i\mathbf{Q}.\mathbf{r}_k]$, the total scattered intensity can be expressed in the following simple form of:

$$\begin{aligned} I(Q) &= I_1 + I_2 + I_3 \quad (6)\\ I_1 &= \rho_m^2 Z(\mathbf{Q})^2\\ I_2 &= \rho_m[A_s(\mathbf{Q})\sum 2\cos(\mathbf{Q}.\mathbf{r}_k)] * |Z(\mathbf{Q})|^2\\ I_3 &= |\{A_s(\mathbf{Q})\exp[-i\mathbf{Q}.\mathbf{r}_k]\} * Z(\mathbf{Q})|^2. \end{aligned}$$

The first sinusoidal term (I_1) describes the classical interference phenomenon of the thin film while the third term characterizes diffraction purely by the metallic clusters. In the case of an incoherent scattering, one can neglect the second term which is a coupled expression. In the following we will use this approximation. We initially consider that the spherical clusters are randomly oriented and distributed throughout the uniform matrix, the heterogeneity are polydisperse in both size and inter-clusters' distances. To calculate the term I_3, we assume that $A_s(\mathbf{Q}).B(\mathbf{Q})$ (in which $B(\mathbf{Q}) = \exp[-i\mathbf{Q}.\mathbf{r}_k]$) has not very sharp maxima; it is legitimate then to make the following approximation: $B(\mathbf{Q}) * Z(\mathbf{Q}) \approx B(\mathbf{Q})$. Following the Wiener-Khintchine theorem, we have $|B(\mathbf{Q})|^2 = TF|W(\mathbf{r})|$ and I_3 is replaced by $I_3 = |A_s(\mathbf{Q})|^2 TF(W(\mathbf{r}))$ with $W(\mathbf{r})$ defined as the position-position auto correlation function:

$$\begin{aligned} W(r) &= \sum\delta(r - r_k) * \sum\delta(r - r_k\prime)\\ &= N_t\delta(r-0) + \delta(r - r_{i,i+1})\delta(r + ri, i+1)\\ &\quad + \ldots\ldots\ldots \delta(r - r_{i,i+m})\delta(r + r_{i,i+m}) \quad (7) \end{aligned}$$

where $r_{i,i+1} = r_i - r_{i+1}$ (distance between the first neighbours) and $r_{i,i+2} = r_i - r_{i+2}$ (distance between the second neighbors). More explicitly, $W(r)$ can be expressed as:

$$W(r) = N_t\{\delta(r) + H_1(r) + H_{-1}(r) + \ldots\ldots\ldots H_m(r) + H_{-m}(r)\} \quad (8)$$

in which N_t is the total number of clusters in the thin granular film and H_m is the distribution function of the mth neighbors. If a Gaussian distribution is considered: $H_1(r) = \exp -[(r - \langle s\rangle)^2/2\sigma_s^2]$, it can be shown that $H_k(r) = H_{k-1}(r) * H_{k-1}(r)$ [14] so that

$$TF\,(W(r)) = \{[1 - \exp(-2Q^2\sigma^2)]/[1 - 2\cos(Q\langle S_c\rangle) \times \exp(-Q^2\sigma^2) + \exp(-2Q^2\sigma^2)]\}. \quad (9)$$

To take into account the total reflection and the variation at very small Q values and as the kinematical approach fails close to the total reflection region, one can substitute the expression I_1 by the well-known Airy's function in classical optics. These previous considerations suggest that the total scattered intensity is formed by two terms:

$$I(\mathbf{Q}) = \left|\frac{[r_{0,1} + r_{1,2}\exp(j2Q_zD)]}{[1 + r_{0,1}r_{1,2}\exp(j2Q_zD)]}\right|^2 + \xi A_s(Q)^2\{[1 - \exp(-2Q^2\sigma^2)]/[1 - 2\cos(Q\langle S_c\rangle) \times \exp(-Q^2\sigma^2) + \exp(-2Q^2\sigma^2)]\} \quad (10)$$

$r_{0,1}$ and $r_{1,2}$ are the reflection coefficients between the substrate and thin film and between the thin film and air, ξ is a normalization factor proportional to the clusters concentration in the granular film. As will be shown, the experimental verification of this scattering formula (pure interference with pure diffraction phenomena by heterogeneity) requires a simulation in three times: (i) simulation of the total reflection plateau and the neighboring region (small Q values), (ii) simulation of the small angle scattering signal due to the Pt clusters mainly in the intermediate Q region and at last (iii) simulation of the two signals in the whole Q range.

3 Experiments

To check the validity of the previous predictions, granular Pt-Al_2O_3 films are studied. These thin films are composed by Pt clusters embedded in an amorphous Al_2O_3 matrix. They are made by the radio-frequency co-sputtering method described elsewhere [15] and deposited on float-glass substrates. The target consists of an Al_2O_3 disc 13 cm in diameter in which circular Pt pellets 5 mm in diameter are disposed in a hexagonal array. This configuration allows to make homogeneous granular films whose composition could be varied over a wide range depending on the number of pellets used. In our case, the number of pellets is fixed to 42 corresponding to Pt volume factor $\chi \approx 0.3$ far from the percolation composition (between 0.4 and 0.5). The metal fraction volume of platinum into the deposited granular Pt-Al_2O_3 film is determined by electron microprobe analysis. The float-glass substrates are fixed on a rotating sample holder to enhance the homogeneity of composition and thickness' uniformity. During deposition, the argon pressure is 7×10^{-3} torr and the deposition rate is about 50 Å/min. The latter value corresponds to film thickness of the order of 600 Å. Moreover, to make clear the effect of Pt heterogeneity buried in the Al_2O_3 matrix, on the reflectivity profiles, pure Pt and pure Al_2O_3 thin film with approximately the same thickness, are prepared under the same condition as the granular Pt-Al_2O_3 film. Moreover, to compare our results with those obtained by the standard small angle X-ray (neutron) scattering method "transmission", a very thick film of granular Pt-Al_2O_3 with the same Pt concentration is deposited on a kapton substrate and tested in transmission mode.

The X-ray reflectivity experiments are performed on a θ-2θ reflectometer of the "Institut d'Optique Théorique et Appliquée" (Fig. 2a). It uses a sealed-tube source ($\lambda =$ 1.5405 Å) and mechanically scans the angle of incidence θ from 0.027 to 5° in steps of 5.5×10^{-3}°. This translates into a momentum range of 0.004 to 0.5 $Å^{-1}$. The beam size typically 40 mm × 10 mm and the sample has a dimension of approximately 40×20 mm^2. Slits aperture of 40 mm and counting times of 10 s per point are chosen to detect as many fringes as possible. To check the reproducibility of the experimental results, the same experiments are performed on the X-ray reflectometers of the "Laboratoire de l'État Condensé–Université du Maine" and European Synchrotron Radiation Facility–Grenoble. Moreover, both specular and non specular reflection scans are performed. One can accentuate on an important point related to the collection of the reflected beam at the detector. As indicated in Figure 2b, the collected intensity is accumulated in short ΔQ_x and ΔQ_z range but large ΔQ_y one, especially, due to the size of the second slit. A knowledge of this is assumed in the following discussions.

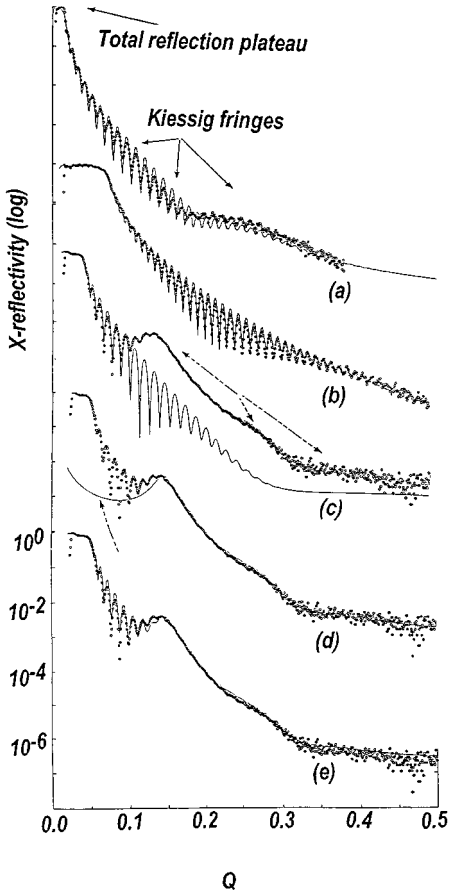

Fig. 3. X-ray reflectivity profiles of (a) 600 Å pure Al_2O_3/float-glass, (b) 600 Å pure platinum Pt/float-glass, (c) 600 Å granular Pt0.3-(Al_2O_3)/float-glass. The circles are the experimental curve, the full line the simulation, calculated with the parameters of Table 1, (d) (Open circles) Experimental X-ray reflectivity profile of the granular film Pt0.3-(Al_2O_3)/ float-glass, (full line) calculated curve of the diffraction part due to small angle scattering by the spherical platinum clusters; (e) (full line) summation of the two intensity contributions (pure film interference + pure correlated scattering Pt clusters.

4 Results and discussion

The experimental data are plotted on a logarithmic scale so that the intensities covering seven orders of magnitude can be observed as shown in Figure 3. In detail, it depicts the X-ray reflectivity profiles given by thin films of pure alumina (Fig. 3a), pure platinum (Fig. 3b) and granular Pt-Al_2O_3 (Fig. 3c). At small grazing angles, the incoming beam is totally reflected giving rise to the plateau of total

Table 1. Simulation parameters of experimental reflectivity curves of the following samples: Al_2O_3 film/float-glass, Pt film/float-glass and Pt 0.3-Al_2O_3 granular cermet film/float-glass.

Sample	Stack nature	Thickness (Å)	Roughness (Å)	$\delta \times 10^6$	$\beta \times 10^6$
Al_2O_3	Interface layer	31.8	6.3	30	2.1
	Pure Al_2O_3 layer	508.0	9.6	25.6	1.6
	Surface layer	16.6	7.9	11.9	20.3
Pt	Pure Pt layer	599.4	8.2	135	13.2
Pt 0.3-Al_2O_3	Homogeneous layer	450	8.2	100	13.2

reflection in each case. Over this region, usual interference fringes so called "Kiessig fringes", due to the finite film thickness, are observed. As it is known, this interference set is originated from interference between the beams partially reflected at the air-film and film-float glass substrate interfaces respectively (Fig. 1). Accurately, the partial reflected beams at these two interfaces interfere with each other depending mainly on the thickness of the different films and the angle of incidence, inducing constructive or destructive interference's. The simulation of total reflection plateau and Kiessig fringes allow to deduce the mean electron density, total thickness and interfacial roughness of each film. Those fit parameters are summarized in Table 1.

One can distinguish that the reflectivity profile of granular Pt-Al_2O_3 film (Fig. 3c) is not completely fitted if we take into account only the interference part due to the finite dimension of the film supposed as a continuous medium. Accurately, there is a great difference between this reflectivity profile and that of pure Al_2O_3 and pure Pt films. The granular Pt-Al_2O_3 film's profile presents not only Kiessig fringes but also another set of sinusoidal fringes for which the intense first peak is roughly located at $Q_z = 0.12$ Å^{-1}. The period of such a system is, approximately, 15 higher than that of the Kiessig fringes. This conforms with more or less an ordered collection with an average periodicity of 45 Å. According to the form of this signal over 0.12 Å^{-1}, one could infer that this corresponds to a small angle scattering by heterogeneity and correlation in their respective spatial arrangements. In that light, judging solely from SAS data, there are mainly two different possible origins for the observed behavior: the first is the platinum clusters surrounded by alumina and the second is the voids in the Al_2O_3 if any. Independent information from other experiments are used to decide between these two different origins; as the granular samples are made by co-sputtering and not by compacting procedures, there is no reason to have voids in such thin films as shown by previous studies [16]. So, the small angle scattering is certainly produced by Pt clusters dispersed in the Al_2O_3 matrix. Assuming the previous model, described in Section 2 (following Eq. (10)), we have considered spherical Pt clusters, characterized by their average diameter $\langle \phi_c \rangle$ and inter-cluster mean distance $\langle S_c \rangle$ embedded in the amorphous alumina with a total film thickness D. The simulation of the small angle scattering part caused by the spherical Pt heterogeneity as shown in Figure 3d (full line) gives the following values: $\langle \phi_c \rangle = 29 \pm 3$ Å, $\langle Sc \rangle = 42 \pm 5$ Å. As underlined earlier (Tab. 1), the simulation of the interference part in Figure 3c (continuous line) due to the thin film interfaces gives a thin film thickness of $D = 450$ Å and an average density (as defined in equation (1), of $\langle \delta_{film} \rangle \approx 10.6 \times 10^{-6}$. The summation of the two intensity contributions allows to fit the experimental reflectivity profile of the granular film as reported in Figure 3e. One can note that there is *a priori* another problem concerning the unicity of the parameters of the fit. Since the contribution of the Pt particles to the total reflectivity curve is more or less smooth function of Q, it could be possible that the values of these free parameters are correlated, *i.e.* another values of size and distance could yield a good fit as well. To overcome this real ambiguity, a comparison with experimental results obtained by other techniques are necessary. In this sense, standard transmission small angle scattering measurements are performed. For this, a thick Pt0.3-Al_2O_3 film (1 mm thickness) on to a pure kapton substrate (6 mm thickness) is investigated. The sample is rolled to have approximately 1 mm thickness. The same procedure with a pure kapton substrate is achieved. Transmission SAS experiments on both samples are performed and, in this way, the small angle scattering signal corresponding to thick Pt-Al_2O_3 film only is obtained by subtraction and background correction (Fig. 4). From the simulation of the SAS spectrum, it is found that the Pt spherical clusters diameter and inter-clusters distance are $\langle \phi_c \rangle = 37 \pm 5$ Å, $\langle S_c \rangle = 44 \pm 12$ Å. In this case, the inter-clusters distance is in comparison with the deduced values of the thinnest preceding Pt-Al_2O_3 granular sample ($\langle S_c \rangle = 42 \pm 5$ Å) while there is a slight difference in the clusters' diameter. The late statement seems to indicate that the morphology of the clusters depends greatly on the film thickness.

Table 2 outlines some results of $\langle \phi_c \rangle$ and $\langle S_c \rangle$, found in literature concerning Pt-Al_2O_3 system [15,16]. Though the results obtained by small X-rays angle scattering in transmission on thick films are more or less in satisfactory agreement with that expected by X-rays reflection mode (on thin films), there is a large difference with the results obtained by transmission electron microscopy. This large disagreement between the present results and those of Sella [15] and Graighead [16] and their co-workers, could be associated, *a priori*, to statistical problems in the measurements of $\langle \phi_c \rangle$ and $\langle S_c \rangle$ or-and film's thickness (the experimented films in Refs. [14,15] were of the order of 4000 Å) and may be to the nature of substrate and deposition conditions.

Table 2. Diameter and inter-cluster distance of platinum clusters in alumina matrix obtained by different experimental methods.

Reference	[15]	[16]	this work thick film	this work thin film
Cluster shape	spherical	spherical	spherical	spherical
$\langle\phi_c\rangle$ (Å)	50	50	37	29
$\langle S_c\rangle$ (Å)	-	-	44	42
σ_f (Å)	-	-	5	3
σ_s (Å)	-	-	12	5
Prepared by	co-sputtering	co-evaporated	co-sputtering	co-sputtering
Investigated by	TEM	TEM	SAXS (in transmission)	X-ray reflectometry

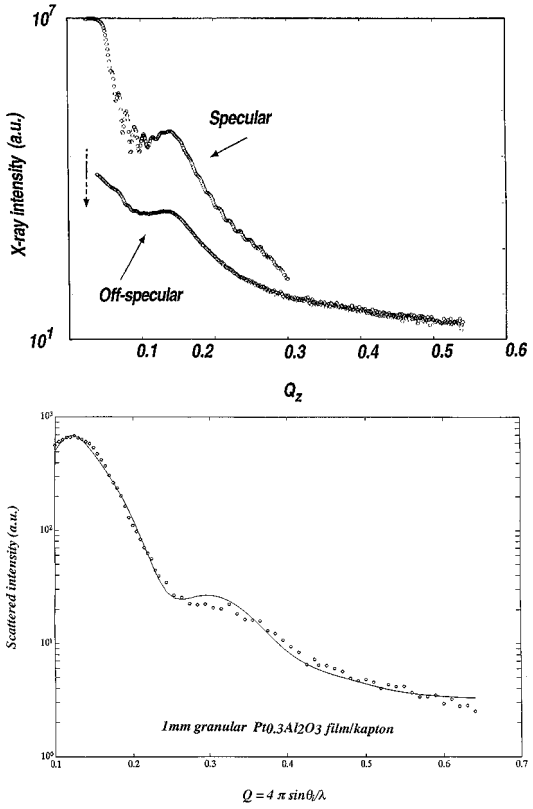

Fig. 4. (Open circles) Experimental X-ray standard small angle scattering (transmission geometry) of a thick granular film Pt0.3-(Al_2O_3) with 1 mm total thickness and its corresponding fit (full line).

One can mention that in the previous simulation of both reflectivity and transmission profiles of granular films, we have considered a two-phase system (Pt clusters and Al_2O_3 matrix) *i.e.* there is no interface between Pt clusters and the alumina matrix. The justification is that platinum is not susceptible to oxidization in forming self-protective PtO_y interface neither $PtAl_x$ (at the deposition temperature).

Now, how can we explain the existence of small angle scattering and pure specular reflection phenomena together, in the grazing angle reflection geometry in the case of granular thin films? Based on the experimental remarks and the model proposed in Section 2, one could suggest a consistent explanation of our experimental findings. The manifestation of the two previous phenomena is related to the continuous and discontinuous behavior of the granular film which is itself related, *a priori*, to the number of Pt clusters. Let us give an estimation of such a number which can be approximated to $NcD/(\sin\theta\langle Sc\rangle)$. For $Q = 0.06$ Å^{-1} (near total reflection region) and 0.4 Å^{-1} (far from total reflection region), N_c is of the order of 1850 and 270 respectively. The corresponding phase shift $\Delta\Phi = 2\pi\langle\phi\rangle N_c(n_c - n_m)/\lambda$ is of the order of 7 and 0.9 radians. Thus, not far from the total reflection plateau, the numbers of platinum clusters crossed by the incident wave is so high that the granular Pt-Al_2O_3 thin film behaves as a continuous and dense medium ($\Delta\Phi < 1$). This could explain the existence of Kiessig fringes, which characterize the continuous behavior of thin films, confirming the preponderance of the refraction phenomenon. By opposite, far from the total reflection region, the number of Pt clusters is low and the granular film exhibits its discontinuous aspect ($\Delta\Phi$ <1). It is obvious that over the total reflection plateau, a competing process between the pure film interference and pure platinum clusters' diffraction is taking place. Moreover, it is reasonable to conclude that the preponderance of one of them depends on the contrast in the electron density (nuclear or magnetic scattering length density for neutrons) between the clusters and the matrix, and also the reflecting amplitude of the substrate.

What about the importance in the future of the possibility to probe heterogeneous thin films by grazing angle X-ray or neutron reflectometry?

(i) First, from a fundamental point of view, although the investigation of the granular Pt-Al_2O_3 thin films was performed in a grazing angle geometry, they exhibit both their continuous and discontinuous aspects.

(ii) Second, from a technical point of view, it is evident that this method presents an advantage to the standard Small Angle Scattering "transmission"; it concerns the sample's thickness required to experiments which is of the order of 1 mm (or more) and of 200 for standard SAS and GAR respectively. Moreover, in this reflection geometry, measurements are not disturbed by the direct transmitted beam which could be a source of background. Compared to Electron Transmission Microscopy, Atomic Force Microscopy and Scanning Tunnelling Microscopy, this method is more accurate regarding the statistical precision on the determination of $\langle S_c\rangle$ and $\langle\phi_c\rangle$ (10^{12} and 10^4 clusters for the proposed method and AFM or TEM respectively).

(iii) Concerning the application field, it is possible to investigate bi-dimensional (compared to the size of clusters) phenomena in very thin heterogeneous films. This method would advance in the importance if neutrons are used; due to the neutron spin, polarized grazing angle neutron reflectometry, in the same geometry as for the previous X-rays study, allows to investigate bi-dimensional magnetism (magnetic domains of the order of 50) and surface superconductivity (flux-lines lattices); an example which could be performed would be the determination of the size and inter-vortices distance in very thin superconductor films as it was done in bulk superconductor materials [17]. Likewise, it could be possible to study superconductivity in the granular thin films because they provide likely candidates for excitonic-induced superconductivity of the type postulated by Ginzburg that might occur at a metal-dielectric interface; no evidence exists for such mechanism at present, although a wide variety of interfaces have been examined [18]. As emphasized earlier, the discussion within this paper was restricted to the application of the proposed method to study granular films dealing essentially with heavy metallic nano-particles embedded in a light matrix; conclusions might be quite different for example, for polymers where the deuteration technique in neutron scattering can be applied.

(iv) There is an additional field where the method to study granular thin films takes its appropriate place; it is related to the non specular reflection of X-rays and neutrons [19]. Effectively, till now, the experimental studies achieved in this domain do not take into account the contribution due to the volume defects which could exist in the studied thin film or multilayered structures as proposed by different authors [20].

5 Conclusion

In the case of granular cermet thin films, it is shown that the observation of the phenomenon of scattering by heterogeneity can be made by using grazing angle reflectivity of X-rays as proposed theoretically by Rauscher and coworkers. This was confirmed by investigating granular thin films of approximately 600 Å thickness, made up by platinum clusters embedded in an alumina matrix. Such an observation of both the interference and diffraction phenomena indicates that the thin granular film exhibits both its continuous and heterogeneous aspects together.

Compared to standard small angle scattering of X-rays or cold neutrons (transmission), the sample's thickness is amply smaller (with a factor of 105), so, 2D phenomena could be studied. The use of dichroic X-rays or polarized neutrons would extend further the possibilities of this method and especially to study surface magnetism and surface superconductivity in heterogeneous very thin films. Likewise, this method could be extrapolated to investigate heterogeneous polymeric thin films with cold neutron reflectometry where the contrast can be improved using isotopic labeling (deuteration-hydrogenation). A comparison between the present model and that developed by Rauscher *et al.* would be very interesting. In addition to the actual samples with an isotropic density fluctuations, we are currently trying to make granular samples presenting a columnar structure to make a serious comparison.

The authors are indebted to Dr. P. Croce for many useful discussions and for the two referees for their judicious suggestions.

References

1. G. Kostorz, in *Treatise on Materials Science & Technology*, edited by G. Kostorz (New York, Academic Press, 1979) Vol. 15, pp. 227-289.
2. A. Guinier, C. R. Acad. Sci. **206**, 1374 (1938); A. Guinier, G. Fournet, in *Small Angle scattering of X-rays* (Wiley, New York, 1955).
3. W.W. Beeman, P. Kaesberg, H.N. Ritland, Phys. Rev. **78**, 336 (1950).
4. O. Kratky, Kolloid. Z. **64**, 213 (1933).
5. H. Rauch, W. Treimer, U. Bonse, Phys. Lett. A **47**, 369 (1974).
6. U. Bonse, M. Hart, Appl. Phys. Lett. **6**, 155 (1965).
7. H. Dosch, Int. J. Mod. Phys. **6**, 2773 (1992) and references therein; H. Dosch, in *Critical Phenomena at Surfaces & Interfaces: Evanescent X-ray and neutron scattering*, in Springer Tracts in Modern Physics (Springer, Heidelberg, 1992) and references therein.
   H. Dosch, T. Hšfer, J. Peisl, R.L. Johnson, Europhys. Lett. **15**, 527 (1991); H. Dosch, J. Peisl, K. Al Usta, Z. Phys. B **79**, 409 (1990).
8. S. Dietrich, A. Haase, Phys. Rep. **260**, (1995) and references therein; S. Dietrich, H. Wagner, Phys. Rev. Lett. **51**, 1469 (1983); S. Dietrich, H.W. Diehl, Z. Phys. B **51**, 343 (1983).
9. T. Salditt, T.H. Metzger, J. Peisl, X. Jiang, L. Phys. **4**, 1573 (1994); T. Salditt, T.H. Metzger, J. Peisl, Phys. Rev. Lett. **73**, 2228 (1994).
10. J.R. Levine, J.B. Cohen, Y.W. Chung, P. Georgopoulos, J. Appl. Cryst. **22**, 528 (1989); J.R. Levine, J.B. Cohen, Y.W. Chung, Surf. Sci. **248**, 215 (1991); J.R. Levine, P. Georgopoulos, Y.W. Chung, J.B. Cohen, J. Phys. IV Colloq. France **3**, C8-411 (1993).
11. A. Naudon, T. Slimani, P. Goudeau, J. Appl. Cryst. **24**, 501 (1991), see also A. Naudon, D. Thiaudire, J.J. Arnault, J. Delafond, C. Templier, C.R.A.S.T. **317** (1993).
12. M. Rauscher, T. Salditt, H. Spohn, Phys. Rev. B. **52**, 16855 (1996).
13. T.J. Davis, Acta. Cryst. A **50**, 686 (1994).
14. B.K. Vainshtein, in *Diffraction of X-rays by Chain Molecules* (Elsevier, Amsterdam-London-New York, 1966).
15. C. Sella, T.K. Vien, J. Lafait, S. Berthier, Thin Solid Films **80**, 425 (1982).
16. H.G. Craighead, Proc. Soc. Phot. Opt. Instr. Eng. **40**, 356 (1982).
17. D. Cribier, B. Jacrot, L. Madhav Rao, B. Farnoux, Phys. Lett. **9**, 106 (1964).
18. H.R. Zeller, I. Giaever, Phys. Rev. **181**, 789 (1969).
19. S.K. Sinha, E.B. Sirota, S. Garoff, H.B. Stanley, Phys. Rev. B **38**, 2297 (1988), also A. Steyerl, S.S. Malik, L.R. Iyengar, Physica B **173**, 47 (1991).
20. P. Croce, L. Prod'homme, Rev. Phys. Appl. **12**, 1641 (1977), also J.P. Chauvineau, Y. Chambet, C. Marlire, in *Optical Interference Coatings Proceeding*, edited by F. Abels (1995), pp. 260-267.